3-D RADIATIVE TRANSFER MODELING OF THE EFFECT OF BUBBLE CLOUDS ON REMOTE-SENSING REFLECTANCE

Jacek Piskozub

Institute of Oceanology, Polish Academy of Sciences, Powsta ców Warszawy 55, 81-712 Sopot, Poland; email: <piskozub@iopan.gda.pl>

Dariusz Stramski, Eric Terrill, W. Kendall Melville

Marine Physical Laboratory, Scripps Institution of Oceanography, University of California at San Diego, La Jolla, California 92093, U.S.A

This work was funded by the Office of Naval Research HyCODE Project (grants N00014-99-1-0223 and N00014-02-1-0190)

ABSTRACT

We examined the effect of bubble clouds on remote-sensing reflectance with a 3-D Monte Carlo model of radiative transfer. The geometry of bubble clouds and the concentration and size distribution of bubbles were defined based on acoustical measurements of bubbles in the surface ocean. The light scattering properties of bubble clouds for various void fractions were calculated using Mie theory. We show how the spatial pattern, magnitude, and spectral behavior of remote-sensing reflectance produced by a bubble cloud is changing due to variations in the geometric and optical properties of the bubble cloud and background optical properties of ambient water. For various values of the inherent optical properties of water, we also determined the minimum size of bubble cloud, above which the water-leaving light field can be reasonably well estimated from a 1-D radiative transfer model with a plane-parallel geometry.

INTRODUCTION

Recent advances in remote sensing technology will soon provide the opportunity to observe ocean color and sea surface phenomena, including whitecap coverage, with hyperspectral radiometric sensors operating within the visible spectral region from the near UV to near IR. This new generation of ocean color sensors will also have an increased spatial resolution with the pixel size of the order of tens of meters. The water-leaving radiance (L_w) and remote-sensing reflectance (RSR) obtained from such observations will be influenced by variability associated with whitecaps and underwater bubble clouds occurring at sub-pixel spatial scales. In this study we describe the preliminary results obtained from 3-D Monte Carlo simulations of radiative transfer, which show the variability in RSR produced by bubble clouds.

Also presented as a talk
on Tuesday, November 19 at 2:50 p.m

MODELING

3-D Monte Carlo code of radiative transfer was used for the modeling. The light scattering properties of bubble clouds were derived from Mie scattering calculations. The Mie calculations were made for six different size distributions of bubbles based on data collected during the HyCODE 2000 experiment. Each size distribution was representative of a specific range of void fraction in seawater, namely 10^{-9}-10^{-8}, 10^{-8}-10^{-7}, 10^{-7}-10^{-6}, 10^{-6}-10^{-5}, 10^{-5}-10^{-4}, and 10^{-4}-10^{-3}. In addition to scattering by bubbles, we used the following components of the inherent optical properties (IOPs) of seawater in our radiative transfer simulations: (i) absorption by pure seawater (Smith and Baker 1981 for 300-330nm, Sogandares and Fry 1997 for 340-370 nm, Pope and Fry 1997 for 380-700 nm, and Smith and Baker 1981 for wavelengths longer than 700 nm, (ii) scattering by pure seawater (Smith and Baker 1981), and (iii) particulate and CDOM absorption and scattering parameterized in terms of chlorophyll concentration (Morel 1991). The scattering phase function of suspended particles for turbid waters was taken from Petzold (1972).

In the initial runs of the Monte Carlo code, we used a model of the bubble cloud consisting of 20 semi-spherical concentric layers with scattering coefficient increasing inward up to 20 m^{-1} for the inner core layer. The inner core had a radius of 1.5 m. Subsequent Monte Carlo runs were made for 20 concentric, vertically-oriented cylindrical layers, which extended from the sea surface to a depth of 2 m. The third cloud model is a homogeneous vertically oriented cylinder of variable radius, depth, and scattering coefficient.

The grid for calculating L_w was usually 35 by 35 square elements, representing the ocean surface area of either 50 m by 50 m or 15 m by 15 m, depending on the size of the bubble cloud. For the spectral modeling, we used the following wavelengths, which correspond mostly to SeaWiFS and MODIS bands: 300, 412, 443, 493, 510, 531, 551, 600, 667, 678, 748, 765, and 800 nm. No inelastic radiative processes (fluorescence, Raman scattering) were considered in our modeling.

RESULTS

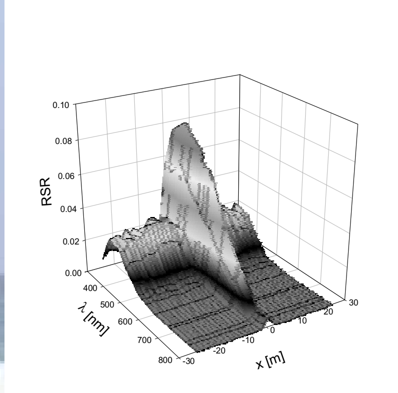

Figure 1. Remote-sensing reflectance across a bubble cloud (x axis) as a function of light wavelength. Semi-spherical cloud model. Water IOPs correspond to chlorophyll concentration of 0 mg/m³, meaning that the 'background' IOPs are defined by absorption and scattering by pure seawater. No inelastic scattering.

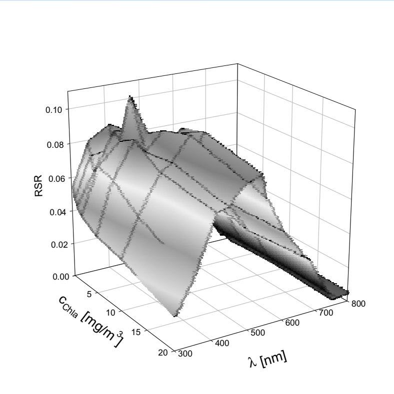

Figure 2. Remote-sensing reflectance just above the center of the bubble cloud as a function of light wavelength and chlorophyll concentration. These results were obtained for a semi-spherical model of the bubble cloud.

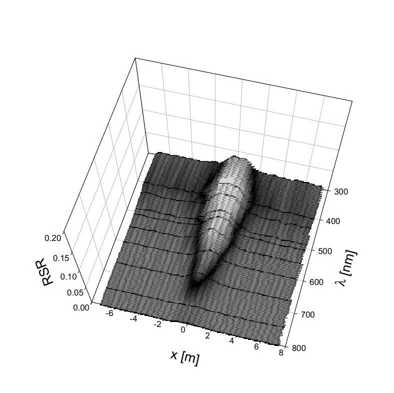

Figure 3. Remote-sensing reflectance across the bubble cloud (x-axis) as a function of light wavelength for a cylindrical model of the cloud as described in the text. The radius of the inner core of the cloud is r = 1 m and the scattering coefficient of bubbles within the inner core is b = 20 m^{-1}. The 'background' IOPs of seawater correspond to the chlorophyll concentration of 1 mg m^{-3}. The spectrally variable footprint size of the bubble cloud may influence the spatially-averaged reflectance to varying extent at different wavelengths if the bubble cloud is on or near the border of the pixel over which the spatial averaging is performed. This effect increases with decreasing pixel size.

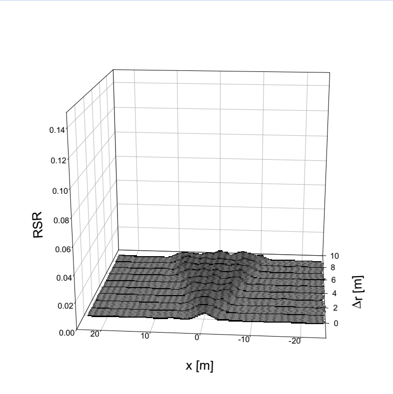

Figure 4. Remote-sensing reflectance across the bubble cloud (x-axis) as a function of the radius of the inner dense core of the cloud. These results were obtained for a cylindrical model of the bubble cloud for the light wavelength of 800 nm and the chlorophyll concentration of 1 mg m^{-3}. Note the 'rim' effect, which is observed here due to the high value of the absorption coefficient (> 2 m^{-1}) at 800 nm. This effect is caused by side illumination of a bubble cloud with sharply defined border in highly absorbing water.

CONCLUSIONS

The variability in the Mie-derived phase functions of bubbles at different void fractions influences significantly the remote-sensing reflectance. This creates the need for using the different phase functions for different regions of the modeled bubble cloud, depending on the local void fraction.

The RSR values over a bubble cloud do not decline to a negligible level in the near infrared.

The size (or the spatial extent) of the RSR pattern above the bubble cloud varies with the attenuation coefficient of seawater. This will have implications for spectral observations such that the bubble cloud will appear larger in terms of the spatial extent of the RSR pattern at wavelengths where absorption is relatively low (typically in the blue-green spectral region).

For certain conditions of the bubble cloud geometry and optical properties, the RSR pattern above the bubble cloud is characterized by a plateau, which suggests that a simpler 1-D model may provide a satisfactory approach to radiative transfer simulations.

REFERENCES

Morel A., "Light and marine photosynthesis : a spectral model with geochemical and climatological implications". Prog. Oceanogr., **26**, 263-306 (1991).
T. J. Petzold, "Volume scattering functions for selected ocean waters", SIO Ref. 72-78, Scripps Institute of Oceanography, U. California, San Diego (1972).
R. M. Pope and E. S. Fry, "Absorption spectrum (380-700 nm) of pure water. II. Integrating cavity measurements," Appl. Opt. **36**, 8710-8723 (1997).
R. C. Smith and K. S. Baker, "Optical properties of the clearest natural waters (200-800 nm)", Appl. Opt. **20**, 177-184 (1981).
F. M. Sogandares and E. S. Fry, "Absorption spectrum (340-700 nm) of pure water. I. Photothermal measurements ", Appl. Optics 36(33), 8699-8709 (1997).